

# Influence of the Cis Ligand on the H–H Separation and the Rotation Barrier of the Dihydrogen in Osmium-Elongated Dihydrogen Complexes Containing an Ortho-Metalated Ketone<sup>†</sup>

Pilar Barrio,<sup>‡</sup> Miguel A. Esteruelas,<sup>\*,‡</sup> Agustí Lledós,<sup>\*,§</sup> Enrique Oñate,<sup>‡</sup> and Jaume Tomàs<sup>§</sup>

Departamento de Química Inorgánica, Instituto de Ciencia de Materiales de Aragón, Universidad de Zaragoza-CSIC, 50009 Zaragoza, Spain, and Unitat de Química Física, Departament de Química, Universitat Autònoma de Barcelona, 08193 Bellaterra, Barcelona, Spain

Received October 22, 2003

Treatment of the complex  $\text{OsH}_3\{\text{C}_6\text{H}_4\text{C}(\text{O})\text{CH}_3\}(\text{P}^i\text{Pr}_3)_2$  (**1**) with  $\text{HBF}_4 \cdot \text{OEt}_2$  in diethyl ether–acetone (2:1) affords the elongated dihydrogen derivative  $[\text{Os}\{\text{C}_6\text{H}_4\text{C}(\text{O})\text{CH}_3\}(\eta^2\text{-H}_2)\{\eta^1\text{-(CH}_3)_2\text{CO}\}(\text{P}^i\text{Pr}_3)_2]\text{BF}_4$  (**2**), which reacts with NaCl and CsF to give  $[\text{Os}\{\text{C}_6\text{H}_4\text{C}(\text{O})\text{CH}_3\}\text{X}(\eta^2\text{-H}_2)(\text{P}^i\text{Pr}_3)_2]$  (X = Cl (**3**), F (**4**)). The X-ray diffraction studies on **2** and **4** and DFT calculations on the model complexes  $\text{OsH}_3\{\text{C}_6\text{H}_4\text{C}(\text{O})\text{CH}_3\}(\text{PH}_3)_2$  (**1t**),  $[\text{Os}\{\text{C}_6\text{H}_4\text{C}(\text{O})\text{CH}_3\}(\eta^2\text{-H}_2)(\text{H}_2\text{O})(\text{PH}_3)_2]^+$  (**2t**), and  $[\text{Os}\{\text{C}_6\text{H}_4\text{C}(\text{O})\text{CH}_3\}\text{X}(\eta^2\text{-H}_2)(\text{PH}_3)_2]$  (X = Cl (**3t**), F (**4t**)) suggest that one of the hydrogen atoms bonded to the osmium atom undergoes a cis electrostatic attraction with the L ligand (L = H (**1**, **1t**),  $(\text{CH}_3)_2\text{CO}$  or  $\text{H}_2\text{O}$  (**2**, **2t**), Cl (**3**, **3t**), F (**4**, **4t**)), which increases in the sequence  $(\text{CH}_3)_2\text{CO}$  or  $\text{H}_2\text{O} < \text{Cl} \leq \text{F} < \text{H}$ . This interaction provokes a lengthening of the hydrogen–hydrogen bond and an increase in the rotation barrier of the elongated dihydrogen ligand. Thus, it is observed that the separation between the hydrogen atoms of the dihydrogen decreases in the sequence **1t** (1.695 Å) > **4t** (1.544 Å) > **3t** (1.489 Å) > **2t** (1.455 Å), whereas the rotation barrier of the dihydrogen increases in the sequence **2** (<9 kcal·mol<sup>-1</sup>) < **3** ( $\approx$ 9 kcal·mol<sup>-1</sup>) < **4** (10.1 ± 0.8 kcal·mol<sup>-1</sup>) < **1** (13.9 ± 0.3 kcal·mol<sup>-1</sup>).

## Introduction

The coordination of molecular hydrogen to an asymmetrical metallic fragment promotes the polarization of the hydrogen–hydrogen bond. Thus, one of the hydrogen centers of the coordinated H<sub>2</sub> is positively charged.<sup>1</sup> In *cis*-hydride–dihydrogen complexes, it has been recognized that the coordinated H<sub>2</sub> ligand has the capability of interacting with the hydride. Theoretical studies have not characterized any form of covalent bonding between the hydride and the dihydrogen. The bonding is described as an electrostatic attraction or a dipole/induced dipole interaction between the negatively

charged hydride and the positively charged extremity of the coordinated H<sub>2</sub>.<sup>1d,f,g</sup> From an electronic point of view the situation seems to be similar to that in the hydrogen bond.<sup>2</sup> This interaction provokes structural distortions in the coordination of the dihydrogen and perturbations in its rotation barrier.<sup>3</sup>

Elongated dihydrogen complexes are a group of dihydrogen compounds with the hydrogen–hydrogen separation ranging from 1.0 to 1.6 Å. They present as a distinctive characteristic a very flat energy potential curve for the H–H stretch.<sup>4</sup> In such a situation small perturbations, like those caused by weak interactions, could induce severe changes in the H···H distance. Thus, this kind of dihydrogen complex is very sensitive to detection and comparison of the strength of weak interactions involving the H<sub>2</sub> unit.

The osmium complexes of this type have been shown to be useful templates for carbon–carbon and carbon–heteroatom coupling reactions.<sup>5</sup> However, their reactivity toward unsaturated organic molecules is difficult to

\* To whom correspondence should be addressed. E-mail: maester@posta.unizar.es (M.A.E.).

<sup>†</sup> Dedicated to Prof. Helmut Werner on the occasion of his 70th birthday.

<sup>‡</sup> Universidad de Zaragoza-CSIC.

<sup>§</sup> Universitat Autònoma de Barcelona.

(1) (a) Jessop, P. G.; Morris, R. H. *Coord. Chem. Rev.* **1992**, *121*, 155. (b) Kristjánssdóttir, S. S.; Norton, J. R. In *Transition Metal Hydrides*; Dedieu, A., Ed.; VCH: New York, 1992; pp 309–359. (c) Jia, G.; Lau, C.-P. *Coord. Chem. Rev.* **1999**, *190–192*, 83. (d) Maseras, F.; Lledós, A.; Clot, E.; Eisenstein, O. *Chem. Rev.* **2000**, *100*, 601. (e) Abdur-Rashid, K.; Fong, T. P.; Greaves, B.; Gusev, D. G.; Hinman, J. G.; Landau, S. E.; Lough, A. J.; Morris, R. H. *J. Am. Chem. Soc.* **2000**, *122*, 9155. (f) Kubas, G. J. *J. Organomet. Chem.* **2001**, *635*, 37. (g) Kubas, G. J. *Metal Dihydrogen and  $\sigma$ -Bond Complexes*; Kluwer Academic/Plenum: New York, 2001.

(2) (a) Richmond, T. G. *Coord. Chem. Rev.* **1990**, *105*, 221. (b) Peris, E.; Lee, J. C., Jr.; Rambo, J. R.; Eisenstein, O.; Crabtree, R. H. *J. Am. Chem. Soc.* **1995**, *117*, 3485. (c) Crabtree, R. H. *J. Organomet. Chem.* **1998**, *557*, 111. (d) Crabtree, R. H.; Eisenstein, O.; Sini, G.; Peris, E. *J. Organomet. Chem.* **1998**, *567*, 7. (e) Custelcean, R.; Jackson, J. E. *Chem. Rev.* **2001**, *101*, 1963.

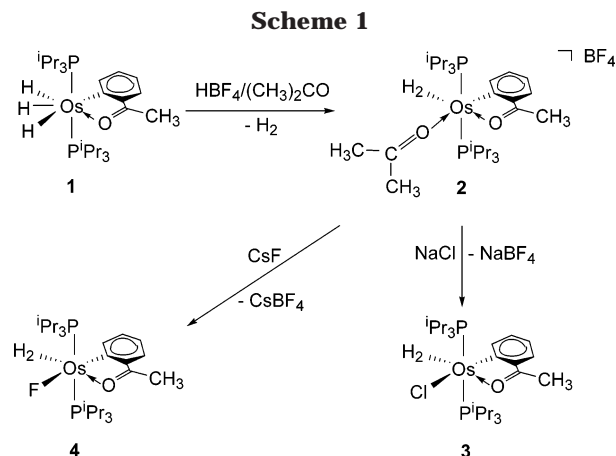
rationalize.<sup>6</sup> The products of the reactions of  $L_n\text{Os}$ - $(\text{H}\cdots\text{H})$  with alkynes appear to depend on the interactions within the  $\text{OsH}_2$  unit,<sup>7</sup> which are determined by the electronic structure of the  $L_n\text{Os}$  fragment.<sup>8</sup>

Our interest in learning to rationalize the reactivity of the elongated dihydrogen complexes toward alkynes prompted us to prepare *cis*- $L$ -dihydrogen complexes of

the general formula  $\text{Os}\{\text{C}_6\text{H}_4\text{C}(\text{O})\text{CH}_3\}L(\eta^2\text{-H}_2)(\text{P}^i\text{Pr}_3)_2$  and to study the influence of the  $L$  ligand on various parameters, depending on the  $\text{MH}_2$  interactions.

## Results and Discussion

**1. Preparation of the Complexes.** The complexes have been prepared according to the reaction sequence shown in Scheme 1.



Treatment at room temperature of the previously reported trihydride  $\text{OsH}_3\{\text{C}_6\text{H}_4\text{C}(\text{O})\text{CH}_3\}(\text{P}^i\text{Pr}_3)_2$  (**1**)<sup>9</sup> in diethyl ether–acetone (2:1) with 1.2 equiv of  $\text{HBF}_4\cdot\text{OEt}_2$  affords the cationic elongated dihydrogen derivative

$[\text{Os}\{\text{C}_6\text{H}_4\text{C}(\text{O})\text{CH}_3\}(\eta^2\text{-H}_2)\{\eta^1\text{-(CH}_3)_2\text{CO}\}(\text{P}^i\text{Pr}_3)_2]\text{BF}_4$  (**2**), as a result of the protonation of one of the hydride ligands of **1** and the coordination of an acetone molecule. Complex **2** was isolated as an orange solid in 81% yield. The coordination of the oxygen atom of acetone to the osmium atom is strongly supported by the  $^{13}\text{C}\{^1\text{H}\}$  NMR and IR spectra. The  $^{13}\text{C}\{^1\text{H}\}$  NMR spectrum at 253 K in dichloromethane- $d_2$  contains a singlet at 220.0 ppm for the carbon atom of the carbonyl group of acetone, whereas the IR spectrum in Nujol shows the  $\nu(\text{CO})$  band at  $1711\text{ cm}^{-1}$ . In addition, also worthy of note are the absorption due to the  $[\text{BF}_4]^-$  anion with  $T_d$  symmetry centered at  $1050\text{ cm}^{-1}$  and the  $\nu(\text{Os}-\text{H})$  absorption at  $2183\text{ cm}^{-1}$ .

The acetone ligand of **2** can be readily displaced by chloride and fluoride. The substitution is facilitated by the weakness of the  $\text{Os}$ –acetone bond. The addition of 1.2 equiv of  $\text{NaCl}$  to a methanol solution of **2** results in

the precipitation of  $\text{Os}\{\text{C}_6\text{H}_4\text{C}(\text{O})\text{CH}_3\}\text{Cl}(\eta^2\text{-H}_2)(\text{P}^i\text{Pr}_3)_2$  (**3**), as a red solid in 76% yield, whereas the treatment of a tetrahydrofuran solution of **2** with 1.5 equiv of  $\text{CsF}$

affords  $\text{Os}\{\text{C}_6\text{H}_4\text{C}(\text{O})\text{CH}_3\}\text{F}(\eta^2\text{-H}_2)(\text{P}^i\text{Pr}_3)_2$  (**4**), as a red solid in 57% yield. In the IR spectra in Nujol of **3** and **4**, the most noticeable feature is the presence of  $\nu(\text{Os}-\text{H})$  absorptions at  $2187$  (**3**) and  $2147\text{ cm}^{-1}$  (**4**). The presence of a fluoride ligand in **4** is strongly supported by the  $^{19}\text{F}$  NMR spectrum of this compound in benzene- $d_6$ , which at room temperature shows at  $-360.4\text{ ppm}$  a triplet of triplets with  $\text{F}-\text{P}$  and  $\text{F}-\text{H}$  coupling constants of 26.6 and 18.3 Hz, respectively.

**2. Structures.** Complexes **2** and **4** have been characterized by X-ray diffraction analysis.

An ORTEP drawing of the structure of the cation of **2** is presented in Figure 1. Selected bond distances and angles are listed in Table 1. The coordination geometry around the osmium atom could be rationalized as being derived from a distorted octahedron with the two

(3) See for example: (a) Johnson, T. J.; Huffman, J. C.; Caulton, K. G.; Jackson, S. A.; Eisenstein, O. *Organometallics* **1989**, *8*, 2073. (b) Van Der Sluys, L. S.; Eckert, J.; Eisenstein, O.; Hall, J. H.; Huffman, J. C.; Jackson, S. A.; Koetzle, T. F.; Kubas, G. J.; Vergamini, P. J.; Caulton, K. G. *J. Am. Chem. Soc.* **1990**, *112*, 4831. (c) Jackson, S. A.; Eisenstein, O. *Inorg. Chem.* **1990**, *29*, 3910. (d) Jackson, S. A.; Eisenstein, O. *J. Am. Chem. Soc.* **1990**, *112*, 7203. (e) Maseras, F.; Duran, M.; Lledós, A.; Bertrán, J. *J. Am. Chem. Soc.* **1991**, *113*, 2879. (f) Chaudret, B.; Chung, G.; Eisenstein, O.; Jackson, S. A.; Lahoz, F. J.; López, J. A. *J. Am. Chem. Soc.* **1991**, *113*, 2314. (g) Riehl, J.-F.; Péliissier, M.; Eisenstein, O. *Inorg. Chem.* **1992**, *31*, 3344. (h) Albinati, A.; Bakhmutov, V. I.; Caulton, K. G.; Clot, E.; Eckert, J.; Eisenstein, O.; Gusev, D. G.; Grushin, V. V.; Hauger, B. E.; Klooster, W. T.; Koetzle, T. F.; McMullan, R. K.; O'Loughlin, T. J.; Péliissier, M.; Ricci, J. S.; Sigalas, M. P.; Vymenits, A. B. *J. Am. Chem. Soc.* **1993**, *115*, 7300. (i) Bianchini, C.; Masi, D.; Peruzzini, M.; Casarin, M.; Maccato, C.; Rizzi, G. A. *Inorg. Chem.* **1997**, *36*, 1061. (j) Rodríguez, V.; Sabo-Etienne, S.; Chaudret, B.; Thoburn, J.; Ulrich, S.; Limbach, H.-H.; Eckert, J.; Barthelat, J.-C.; Hussein, K.; Marsden, C. J. *Inorg. Chem.* **1998**, *37*, 3475. (k) Bayse, C. A.; Hall, M. B.; Pleune, B.; Poli, R. *Organometallics* **1998**, *17*, 4309. (l) Soubra, C.; Chan, F.; Albright, T. A. *Inorg. Chim. Acta* **1998**, *272*, 95. (m) Borowski, A. F.; Donnadiou, B.; Daran, J.-C.; Sabo-Etienne, S.; Chaudret, B. *Chem. Commun.* **2000**, 543.

(4) (a) Collman, J. P.; Wagenknecht, P. S.; Hembre, R. T.; Lewis, N. S. *J. Am. Chem. Soc.* **1990**, *112*, 1294. (b) Chinn, M. S.; Heinekey, D. M. *J. Am. Chem. Soc.* **1990**, *112*, 5166. (c) Brammer, L.; Howard, J. A. K.; Johnson, O.; Koetzle, T. F.; Spencer, J. L.; Stringer, A. M. *J. Chem. Soc., Chem. Commun.* **1991**, 241. (d) Esteruelas, M. A.; Oro, L. A.; Ruiz, N. *Inorg. Chem.* **1993**, *32*, 3793. (e) Esteruelas, M. A.; Lahoz, F. J.; Oro, L. A.; Oñate, E.; Ruiz, N. *Inorg. Chem.* **1994**, *33*, 787. (f) Hasegawa, T.; Li, Z.; Parkin, S.; Hope, H.; McMullan, R. K.; Koetzle, T. F.; Taube, H. *J. Am. Chem. Soc.* **1994**, *116*, 4352. (g) Klooster, W. T.; Koetzle, T. F.; Jia, G.; Fong, T. P.; Morris, R. H.; Albinati, A. *J. Am. Chem. Soc.* **1994**, *116*, 7677. (h) Maltby, P. A.; Schlaf, M.; Steinbeck, M.; Lough, A. J.; Morris, R. H.; Klooster, W. T.; Koetzle, T. F.; Srivastava, R. C. *J. Am. Chem. Soc.* **1996**, *118*, 5396. (i) Gross, C. L.; Young, D. M.; Schultz, A. J.; Girolami, G. S. *J. Chem. Soc., Dalton Trans.* **1997**, 3081. (j) Gelabert, R.; Moreno, M.; Lluch, J. M.; Lledós, A. *J. Am. Chem. Soc.* **1997**, *119*, 9840. (k) Rocchini, E.; Mezzetti, A.; Rügger, H.; Burckhardt, U.; Gramlich, V.; Del Zotto, A.; Martinuzzi, P.; Rigo, P. *Inorg. Chem.* **1997**, *36*, 711. (l) Chin, R. M.; Barrera, J.; Dubois, R. H.; Helberg, L. E.; Sabat, M.; Bartucz, T. Y.; Lough, A. J.; Morris, R. H.; Harman, W. D. *Inorg. Chem.* **1997**, *36*, 3553. (m) Barea, G.; Esteruelas, M. A.; Lledós, A.; López, A. M.; Oñate, E.; Tolosa, J. I. *Organometallics* **1998**, *17*, 4065. (n) Barea, G.; Esteruelas, M. A.; Lledós, A.; López, A. M.; Tolosa, J. I. *Inorg. Chem.* **1998**, *37*, 5033. (o) Moehring, G. A.; Williams, C. C.; Buford, J.; Kaviani, M.; Sulko, J.; Fanwick, P. E. *Inorg. Chem.* **1998**, *37*, 3848. (p) Gelabert, R.; Moreno, M.; Lluch, J. M.; Lledós, A. *J. Am. Chem. Soc.* **1998**, *120*, 8168. (q) Torres, L.; Gelabert, R.; Moreno, M.; Lluch, J. M. *J. Phys. Chem.* **2000**, *104*, 7898. (r) Liut, S. H.; Lo, S. T.; Wen, T. B.; Williams, I. D.; Zhou, Z. Y.; Lau, C. P.; Jia, G. *Inorg. Chim. Acta* **2002**, *334*, 122. (s) Esteruelas, M. A.; García-Yebra, C.; Oliván, M.; Oñate, E.; Tajada, M. A. *Organometallics* **2002**, *21*, 1311. (t) Torres, L.; Gelabert, R.; Giménez, X.; Moreno, M.; Lluch, J. M. *J. Chem. Phys.* **2002**, *117*, 7094. (u) Pons, V.; Heinekey, D. M. *J. Am. Chem. Soc.* **2003**, *125*, 8428.

(5) Esteruelas, M. A.; López, A. M. In *Recent Advances in Hydride Chemistry*; Elsevier: Amsterdam, 2001; Chapter 7, pp 189–248.

(6) Esteruelas, M. A.; García-Yebra, C.; Oliván, M.; Oñate, E. *Organometallics* **2000**, *19*, 3260 and references therein.

(7) (a) Esteruelas, M. A.; Lahoz, F. J.; Oñate, E.; Oro, L. A.; Valero, C.; Zeier, B. *J. Am. Chem. Soc.* **1995**, *117*, 7935. (b) Bohanna, C.; Callejas, B.; Edwards, A. J.; Esteruelas, M. A.; Lahoz, F. J.; Oro, L. A.; Ruiz, N.; Valero, C. *Organometallics* **1998**, *17*, 373. (c) Barrio, P.; Esteruelas, M. A.; Oñate, E. *Organometallics* **2002**, *21*, 2491. (d) Barrio, P.; Esteruelas, M. A.; Oñate, E. *Organometallics* **2003**, *22*, 2472.

(8) Castarlenas, R.; Esteruelas, M. A.; Gutiérrez-Puela, E.; Jean, Y.; Lledós, A.; Martín, M.; Tomás, J. *Organometallics* **1999**, *18*, 4296 and references therein.

(9) Barrio, P.; Castarlenas, R.; Esteruelas, M. A.; Lledós, A.; Maseras, F.; Oñate, E.; Tomás, J. *Organometallics* **2001**, *20*, 442.

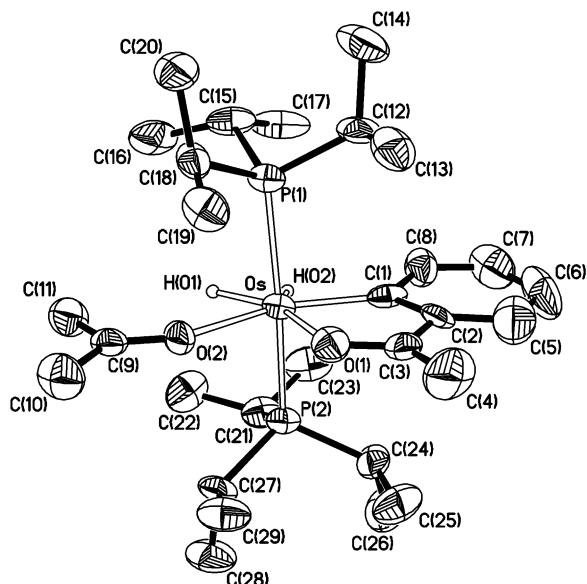


**Figure 1.** Molecular diagram of the cation of the complex  $[\text{Os}\{\text{C}_6\text{H}_4\text{C}(\text{O})\text{CH}_3\}(\eta^2\text{-H}_2)\{\eta^1\text{-(CH}_3)_2\text{CO}\}(\text{P}^i\text{Pr}_3)_2]\text{BF}_4$  (**2**).

**Table 1.** Selected Bond Distances (Å) and Lengths (deg) for the Complex

$[\text{Os}\{\text{C}_6\text{H}_4\text{C}(\text{O})\text{CH}_3\}(\eta^2\text{-H}_2)\{\eta^1\text{-(CH}_3)_2\text{CO}\}(\text{P}^i\text{Pr}_3)_2]\text{BF}_4$ ( <b>2</b> )			
Os–P(1)	2.396(2)	O(2)–C(9)	1.224(9)
Os–P(2)	2.390(2)	C(1)–C(2)	1.377(10)
Os–O(1)	2.115(5)	C(2)–C(3)	1.426(11)
Os–O(2)	2.144(5)	C(3)–C(4)	1.499(12)
Os–C(1)	2.010(8)	Os–H(01)	1.44(4)
O(1)–C(3)	1.244(9)	Os–H(02)	1.50(4)
		H(01)–H(02)	1.49(6)
P(1)–Os–P(2)	171.03(7)	O(1)–Os–H(1)	155(2)
P(1)–Os–O(1)	93.36(14)	O(1)–Os–H(2)	148(2)
P(1)–Os–O(2)	90.06(16)	O(2)–Os–C(1)	154.9(3)
P(1)–Os–C(1)	92.98(19)	O(2)–Os–H(1)	76(2)
P(1)–Os–H(1)	88(3)	O(2)–Os–H(2)	130(2)
P(1)–Os–H(2)	98.4(19)	C(1)–Os–H(1)	129(2)
P(2)–Os–O(1)	95.59(14)	C(1)–Os–H(2)	74(2)
P(2)–Os–O(2)	92.12(15)	H(1)–Os–H(2)	55(3)
P(2)–Os–C(1)	88.71(19)	Os–O(1)–C(3)	117.2(6)
P(2)–Os–H(1)	84(3)	Os–O(2)–C(9)	146.9(6)
P(2)–Os–H(2)	73.6(18)	Os–C(1)–C(2)	116.7(6)
O(1)–Os–O(2)	79.1(2)	C(1)–C(2)–C(3)	114.0(8)
O(1)–Os–C(1)	75.9(3)	O(1)–C(3)–C(2)	116.0(8)

phosphorus atoms of the triisopropylphosphine ligands occupying opposite positions ( $\text{P}(1)\text{--Os--P}(2) = 171.03(7)^\circ$ ). The perpendicular plane is formed by the ortho-metallated ketone, which acts with a bite angle of  $75.9(3)^\circ$ , the acetone ligand cis disposed to the oxygen atom of the metallated ketone ( $\text{O}(1)\text{--Os--O}(2) = 79.1(2)^\circ$ ), and the dihydrogen ligand cis disposed to the metallated carbon atom.

The  $\text{Os--O}(1)$  (2.115(5) Å) and  $\text{Os--O}(2)$  (2.144(5) Å) distances are statistically identical, and they are the expected ones for a single bond. The  $\text{O}(1)\text{--C}(3)$  (1.244(9) Å) and  $\text{O}(2)\text{--C}(9)$  (1.224(9) Å) bond lengths are also statistically identical and quite similar to those in acetophenone (1.217 Å)<sup>10</sup> and free acetone (1.20 Å).<sup>11</sup>

(10) 3D Search and Research Using the Cambridge Structural Data Base: Allen, F. H.; Kennard, O. *Chem. Des. Automation News* **1993**, *8*(1), 1, 31.

(11) Allen, P. W.; Bowen, H. J. M.; Sutton, L. E.; Bastiansen, O. *Trans. Faraday Soc.* **1952**, *48*, 991.

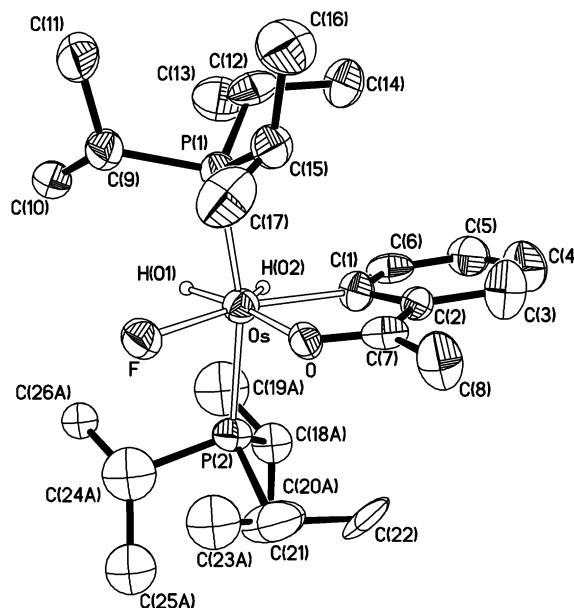


**Figure 2.** Molecular diagram of the complex  $[\text{Os}\{\text{C}_6\text{H}_4\text{C}(\text{O})\text{CH}_3\}\text{F}(\eta^2\text{-H}_2)(\text{P}^i\text{Pr}_3)_2]$  (**4**).

**Table 2.** Selected Bond Distances (Å) and Lengths (deg) for the Complex

$[\text{Os}\{\text{C}_6\text{H}_4\text{C}(\text{O})\text{CH}_3\}\text{F}(\eta^2\text{-H}_2)(\text{P}^i\text{Pr}_3)_2]$ ( <b>4</b> )			
Os–P(1)	2.358(3)	C(1)–C(2)	1.426(10)
Os–P(2)	2.359(3)	C(2)–C(7)	1.437(11)
Os–F	2.048(4)	C(7)–C(8)	1.495(11)
Os–O	2.117(5)	Os–H(01)	1.599(10)
Os–C(1)	2.014(8)	Os–H(02)	1.593(10)
O–C(7)	1.245(10)	H(01)–H(02)	1.34(6)
P(1)–Os–P(2)	167.54(9)	F–Os–C(1)	155.7(3)
P(1)–Os–F	85.05(15)	F–Os–H(1)	93(2)
P(1)–Os–O	91.04(15)	F–Os–H(2)	142(2)
P(1)–Os–C(1)	96.7(3)	O–Os–C(1)	76.6(3)
P(1)–Os–H(1)	90(2)	O–Os–H(1)	172(2)
P(1)–Os–H(2)	100(2)	O–Os–H(2)	137(2)
P(2)–Os–F	85.86(15)	C(1)–Os–H(1)	111(2)
P(2)–Os–O	95.62(15)	C(1)–Os–H(2)	61(2)
P(2)–Os–C(1)	95.1(3)	H(1)–Os–H(2)	50(3)
P(2)–Os–H(1)	82(2)	Os–O–C(7)	118.2(6)
P(2)–Os–H(2)	82(2)	Os–C(1)–C(2)	115.5(6)
F–Os–O	79.2(2)	C(1)–C(2)–C(7)	113.8(8)

The  $\text{Os--C}(1)$  distance of 2.010(8) Å is typical for an  $\text{Os--C}(\text{aryl})$  single bond and agrees well with the values previously found in other ortho-metallated osmium compounds (between 2.06 and 2.14 Å).<sup>12</sup>

Figure 2 shows a view of the molecular geometry of **4**, whereas selected bond distances and angles are collected in Table 2. The coordination polyhedron around the osmium atom is analogous to that of **2** with  $\text{P}(1)\text{--Os--P}(2)$  and  $\text{C}(1)\text{--Os--O}$  angles of 167.54(9) and 76.6(3)°, respectively. The fluorine ligand is cis disposed to

(12) (a) Esteruelas, M. A.; Lahoz, F. J.; López, A. M.; Oñate, E.; Oro, L. A. *Organometallics* **1995**, *14*, 2496. (b) Esteruelas, M. A.; Lahoz, F. J.; Oñate, E.; Oro, L. A.; Sola, E. *J. Am. Chem. Soc.* **1996**, *118*, 89. (c) Buil, M. L.; Esteruelas, M. A.; López, A. M.; Oñate, E. *Organometallics* **1997**, *16*, 3169. (d) Crochet, P.; Esteruelas, M. A.; Gutiérrez-Puebla, E. *Organometallics* **1998**, *17*, 3141. (e) Esteruelas, M. A.; Gutiérrez-Puebla, E.; López, A. M.; Oñate, E.; Tolosa, J. I. *Organometallics* **2000**, *19*, 275. (f) Baya, M.; Crochet, P.; Esteruelas, M. A.; Oñate, E. *Organometallics* **2001**, *20*, 240. (g) Baya, M.; Esteruelas, M. A.; Oñate, E. *Organometallics* **2001**, *20*, 4875. (h) Esteruelas, M. A.; Lledós, A.; Oliván, M.; Oñate, E.; Tajada, M. A.; Ujaque, G. *Organometallics* **2003**, *22*, 3753.



**Table 3. Optimized (B3LYP) Structural Parameters (Å) for the OsH<sub>2</sub>L Unit**

complex	L	d(M–H(02))	d(M–H(01))	d(H(01)–H(02))	d(H(01)–L)	r <sub>vdW</sub> (H)	r <sub>vdW</sub> (L)	r <sub>vdW</sub> (H) + r <sub>vdW</sub> (L)	d(H–L)	gi
<b>1t</b>	H	1.669	1.628	1.695	1.698	1.20	1.20	2.40	0.75	0.42
<b>2t</b>	H <sub>2</sub> O	1.593	1.629	1.455	2.587	1.20	1.52	2.72	1.01	0.08
<b>3t</b>	Cl	1.593	1.616	1.489	2.625	1.20	1.75	2.95	1.25	0.19
<b>4t</b>	F	1.595	1.613	1.544	2.340	1.20	1.47	2.67	0.92	0.19

the oxygen atom of the metalated ketone. The F–Os–O angle is 79.2(2)°.

The Os–F bond length (2.048(4) Å) is about 0.04 Å shorter than the Os–F distances found in the complexes [OsHF(≡CCH<sub>2</sub>Ph)(H<sub>2</sub>p)(P<sup>i</sup>Pr<sub>3</sub>)<sub>2</sub>]BF<sub>4</sub> (2.087(2) Å)<sup>13</sup> and [OsH{F···HON=C(CH<sub>3</sub>)<sub>2</sub>}(≡CCH<sub>2</sub>Cy)(P<sup>i</sup>Pr<sub>3</sub>)<sub>2</sub>]BF<sub>4</sub> (2.085(2) Å),<sup>7c</sup> where F···H hydrogen bonds have been proposed to exist. However, it is about 0.03 Å longer than those found in the dicarbonyl compounds OsF<sub>2</sub>(CO)<sub>2</sub>(PCy<sub>3</sub>)<sub>2</sub> (2.023(4) and 2.022(4) Å) and OsF<sub>2</sub>(CO)<sub>2</sub>(PPh<sub>3</sub>)<sub>2</sub> (2.023(5) Å).<sup>14</sup>

The hydride positions obtained from X-ray diffraction data are, in general, imprecise.<sup>15</sup> However, DFT calculations have been shown to provide useful accurate data for the hydrogen positions in both classical polyhydride and dihydrogen complexes.<sup>1d</sup> Thus, to know the position of the hydrogen atoms of the dihydrogen ligand in the structures of **2** and **4**, DFT studies on the model

complexes [Os{C<sub>6</sub>H<sub>4</sub>C(O)CH<sub>3</sub>}(η<sup>2</sup>-H<sub>2</sub>)(H<sub>2</sub>O)(PH<sub>3</sub>)<sub>2</sub>]<sup>+</sup> (**2t**)

and Os{C<sub>6</sub>H<sub>4</sub>C(O)CH<sub>3</sub>}F(η<sup>2</sup>-H<sub>2</sub>)(PH<sub>3</sub>)<sub>2</sub> (**4t**) have been carried out. In addition, to analyze the influence of the L ligand on the structural parameters of the OsH<sub>2</sub> unit in complexes of the general formula Os{C<sub>6</sub>H<sub>4</sub>C(O)CH<sub>3</sub>}-

L(η<sup>2</sup>-H<sub>2</sub>)(P<sup>i</sup>Pr<sub>3</sub>)<sub>2</sub>, the structures of OsH<sub>3</sub>{C<sub>6</sub>H<sub>4</sub>C(O)CH<sub>3</sub>}-  
(PH<sub>3</sub>)<sub>2</sub> (**1t**) and Os{C<sub>6</sub>H<sub>4</sub>C(O)CH<sub>3</sub>}Cl(η<sup>2</sup>-H<sub>2</sub>)(PH<sub>3</sub>)<sub>2</sub> (**3t**) have been also calculated. The bond distances and angles obtained for the non-hydrogen atoms of **2t** and **4t** agree well with those determined by X-ray diffraction for **2** and **4**.

Figure 3 shows the B3LYP-optimized structures of the four compounds, whereas Table 3 lists the structural parameters for the OsH<sub>2</sub>L unit, as well as the sum of the van der Waals radii of hydrogen and L. As expected, the Os–H distances are about 1.6 Å, and they do not merit any additional comment. However, the separation between the hydrogen atoms of the dihydrogen and the separation between the dihydrogen and L are of great interest.

The H–H separations lie within the range of distances found in the so-called elongated dihydrogen complexes<sup>4</sup> and decrease in the sequence **1t** > **4t** > **3t** > **2t**, whereas the separation between the H(01) hydrogen atom and the L ligand in the four cases is shorter than the sum of the van der Waals radii of hydrogen and L (r<sub>vdW</sub>(H) + r<sub>vdW</sub>(L)).<sup>16</sup>

The values of the H(01)–L separation shown in Table 3 do not have much meaning in themselves. However, one can assume that the sum of the van der Waals radii

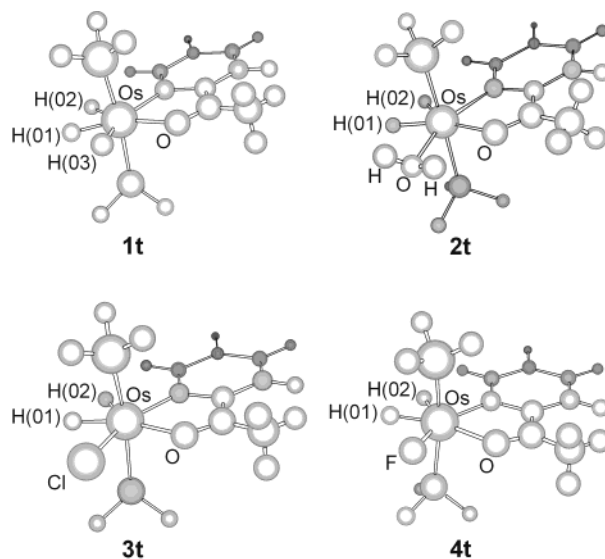


**Figure 3.** Optimized structures at the B3LYP level of theory for the complexes OsH<sub>3</sub>{C<sub>6</sub>H<sub>4</sub>C(O)CH<sub>3</sub>}(PH<sub>3</sub>)<sub>2</sub> (**1t**), [Os{C<sub>6</sub>H<sub>4</sub>C(O)CH<sub>3</sub>}(η<sup>2</sup>-H<sub>2</sub>)(H<sub>2</sub>O)(PH<sub>3</sub>)<sub>2</sub>]<sup>+</sup> (**2t**), and Os{C<sub>6</sub>H<sub>4</sub>C(O)CH<sub>3</sub>}X(η<sup>2</sup>-H<sub>2</sub>)(PH<sub>3</sub>)<sub>2</sub> (X = Cl (**3t**), F (**4t**)).

is the minimum separation between two atoms, which do not form any bond, while the bond distances in free H<sub>2</sub> (0.75 Å), HCl (1.25 Å), HF (0.92 Å) and H<sub>3</sub>O<sup>+</sup> (1.01 Å) correspond to a bond. Then, for each case, one can estimate the extent of H(01)–L interaction (gi) by means of the equation

$$gi = \frac{(r_{vdW}(H) + r_{vdW}(L)) - (d(H(01)–L))}{(r_{vdW}(H) + r_{vdW}(L)) - d(H–L)} \quad (1)$$

where d(H(01)–L) is the separation between H(01) and the L ligand and d(H–L) is the bond distance in free H<sub>2</sub>, HCl, HF, or H<sub>3</sub>O<sup>+</sup>.

The results obtained according to eq 1 (0.42 (**1t**), 0.19 (**4t**), 0.19 (**3t**), 0.08 (**2t**)) show that the grade of H(01)–L interactions increases in the sequence **2t** < **3t** ≈ **4t** < **1t**, as the separation between H(01) and H(02) also increases. This suggests a cis attraction between the H(01) hydrogen atom of the dihydrogen and the L ligand, which lengthens the hydrogen–hydrogen bond. In agreement with the cis interaction, the hydrogen atoms are situated in the same plane as the L ligand and the osmium atom. Because of the electronegative nature of the L ligands and the expected positive partial charge on H(01), it is reasonable to think that this interaction is electrostatic in character. At first glance, one could be surprised at the strength of the interaction in **1t**, which is stronger than those in **3t** and **4t**, where the L ligands (Cl or F) are more electronegative than hydrogen (L = H in **1t**). In this context, it should be noted that in compounds of the general form IrH<sub>2</sub>Y-(pyNPh)(PPh<sub>3</sub>)<sub>2</sub> (Y = H, halogen) the N–H···Y–Ir hydrogen bond is stronger for Y = H than for Y = Cl.

(13) Esteruelas, M. A.; Oliván, M.; Oñate, E.; Ruiz, N.; Tajada, M. *Organometallics* **1999**, *18*, 2953.

(14) Coleman, K. S.; Fawcett, J.; Holloway, J. H.; Hope, E. G.; Russell, D. R. *J. Chem. Soc., Dalton Trans.* **1997**, 3557.

(15) Zhao, D.; Bau, R. *Inorg. Chim. Acta* **1998**, *269*, 162.

(16) The values of the van der Waals radii have been obtained from: Bondi, A. J. *Phys. Chem.* **1964**, *68*, 441.

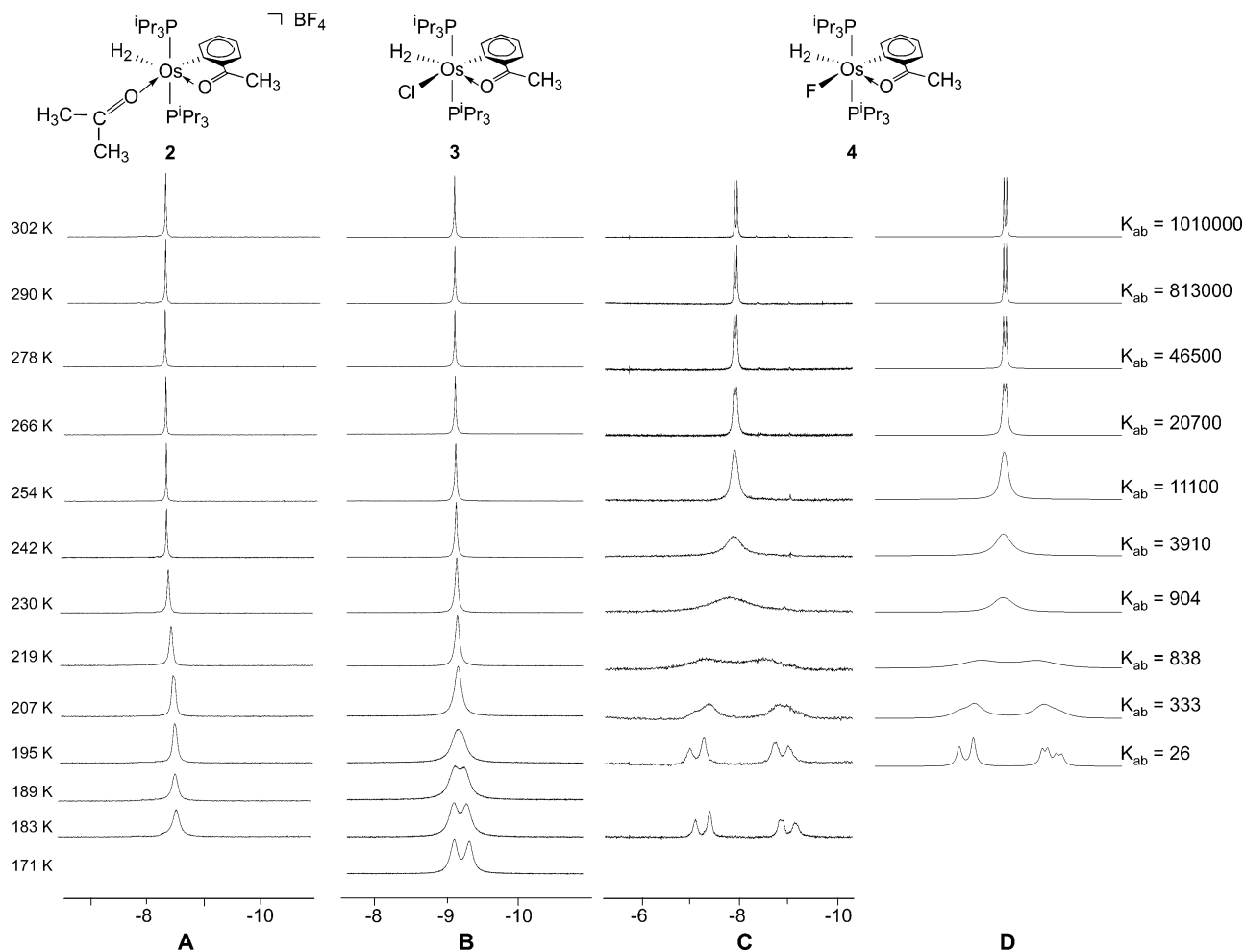


**Figure 4.** Variable-temperature  $^1\text{H}\{^{31}\text{P}\}$  NMR spectra (300 MHz) in the high-field region of  $[\text{Os}\{\text{C}_6\text{H}_4\text{C}(\text{O})\text{CH}_3\}(\eta^2\text{-H}_2)\{\eta^1\text{-}(\text{CH}_3)_2\text{CO}\}(\text{P}^i\text{Pr}_3)_2]\text{BF}_4$  (A),  $\text{Os}\{\text{C}_6\text{H}_4\text{C}(\text{O})\text{CH}_3\}\text{Cl}(\eta^2\text{-H}_2)(\text{P}^i\text{Pr}_3)_2$  (B), and  $\text{Os}\{\text{C}_6\text{H}_4\text{C}(\text{O})\text{CH}_3\}\text{F}(\eta^2\text{-H}_2)(\text{P}^i\text{Pr}_3)_2$  (C) and simulated spectra and rate constants ( $\text{s}^{-1}$ ) for the intramolecular hydrogen site-exchange process of the complex  $\text{Os}\{\text{C}_6\text{H}_4\text{C}(\text{O})\text{CH}_3\}\text{F}(\eta^2\text{-H}_2)(\text{P}^i\text{Pr}_3)_2$  (D).

To rationalize this finding, it has been argued that the Ir–H bond is easily polarized ( $\text{Ir}^{\delta+}\text{-H}^{\delta-}$ ) on the approach of the N–H bond, strengthening the hydrogen-bonding interaction with the latter.<sup>2b</sup>

**3. Rotation Barriers.** At room temperature the  $^{31}\text{P}\{^1\text{H}\}$  NMR spectra of **2** and **3** show a singlet at 12.2 and 10.0 ppm, respectively, whereas the  $^{31}\text{P}\{^1\text{H}\}$  NMR spectrum of **4** contains a doublet at 19.4 ppm, with a P–F coupling constant of 26.6 Hz. These spectra are temperature-invariant between 302 and 183 K. In contrast to the  $^{31}\text{P}\{^1\text{H}\}$  NMR spectra, the  $^1\text{H}$  NMR spectra are temperature-dependent. Figure 4 shows the  $^1\text{H}\{^{31}\text{P}\}$  NMR spectra of **2–4** in the high-field region as a function of the temperature.

The  $^1\text{H}$  NMR spectrum of **2** in dichloromethane- $d_2$  at room temperature shows a broad resonance centered at  $-8.16$  ppm. Lowering the sample temperature produces a broadening of the resonance. However, decoalescence is not observed upon 183 K. At 300 MHz the  $T_1$  values of this resonance were determined over the temperature range 233–183 K. In accordance with the elongated dihydrogen character of the complex, a  $T_1(\text{min})$  value of  $48 \pm 1$  ms was obtained at 193 K. Assuming slow spinning, this value corresponds to a hydrogen–

hydrogen distance of  $1.36 \text{ \AA}$ ,<sup>1a</sup> which is about  $0.1 \text{ \AA}$  shorter than that obtained by DFT calculations.

The  $^1\text{H}$  NMR spectrum of **3** in toluene- $d_8$  at room temperature contains a triplet at  $-8.76$  ppm, with a H–P coupling constant of 11.7 Hz. Lowering the sample temperature leads to broadening of the resonance. At very low temperature (195 K) decoalescence occurs, and at 171 K, two broad signals are clearly observed. In this case, the  $T_1$  values were determined over the temperature range 283–173 K. The  $T_1(\text{min})$  value ( $50 \pm 1$  ms) was obtained at 193 K. It corresponds to a hydrogen–hydrogen distance of  $1.36 \text{ \AA}$ .

The treatment of **3** with methanol- $d_4$  yields the partially deuterated derivative  $\text{Os}\{\text{C}_6\text{H}_4\text{C}(\text{O})\text{CH}_3\}\text{Cl}(\eta^2\text{-HD})(\text{P}^i\text{Pr}_3)_2$  (**3-d**), which has a H–D coupling constant of 4.5 Hz. According to eq 2,<sup>4b</sup> this value allows the calculation of a hydrogen–hydrogen separation of  $1.35 \text{ \AA}$ , which agrees well with that calculated from the  $T_1(\text{min})$  value.

$$d(\text{H-H}) = -0.0167[J(\text{H-D})] + 1.42 \quad (2)$$

The behavior of the  $\text{OsH}_2$  resonance of **3** with changes in temperature indicates that the rotation of the elon-

gated dihydrogen ligand can be blocked on the NMR time scale. A  $\Delta G_{195}^\ddagger$  value of about 9 kcal·mol<sup>-1</sup> can be estimated as the rotation barrier, on the basis of the spectra shown in Figure 4B. A similar phenomenon has

been previously observed for the complex  $\text{Os}\{\text{NH}=\text{C}(\text{Ph})\text{C}_6\text{H}_4\}\text{Cl}(\eta^2\text{-H}_2)(\text{P}^i\text{Pr}_3)_2$ . In this case, the estimated barrier for the H<sub>2</sub> rotation is 12 kcal·mol<sup>-1</sup>.<sup>4m</sup>

Metallocene complexes of the type  $\text{M}(\eta^5\text{-C}_5\text{R}_5)_2(\eta^2\text{-H}_2)\text{L}$  (M = Nb, Ta; L = PR<sub>3</sub>, CO, CNR) also show blocked rotation of the dihydrogen ligand on the NMR time scale. In agreement with the osmium systems the free energy of activation of the H<sub>2</sub> internal rotation is in the range 8–12 kcal·mol<sup>-1</sup>.<sup>17</sup>

The <sup>1</sup>H NMR spectrum of **4** in toluene-*d*<sub>8</sub> at room temperature shows a double triplet at -7.71 ppm with H–F and H–P coupling constants of 18.3 and 12.6 Hz, respectively. Lowering the sample temperature leads to broadening of the resonance. At 219 K, decoalescence occurs, and at 183 K the AB part of an ABXY<sub>2</sub> (X = F, Y = P) spin system is observed. The ABXY<sub>2</sub> spin system is defined by the parameters  $\delta_A - 7.29$ ,  $\delta_B - 9.17$ ,  $J_{AB} = 98$  Hz,  $J_{AX} = 0$  Hz,  $J_{BX} = 37$  Hz, and  $J_{AY} = J_{BY} = 12.6$  Hz. The value of the  $J_{AB}$  coupling constant is temperature-invariant. The <sup>1</sup>H{<sup>31</sup>P} NMR spectra (Figure 4C) are simplified to the expected ABX spin system.

To estimate the separation between the hydrogen atoms of the dihydrogen, the  $T_1$  values of the aforementioned resonance were determined over the temperature range 233–193 K. A  $T_1$ (min) value of  $64 \pm 2$  ms was obtained before the decoalescence, at 223 K. It corresponds to a hydrogen–hydrogen distance of 1.42 Å.

Similarly to **3**, the treatment of **4** with methanol-*d*<sub>4</sub> affords  $\text{Os}\{\text{C}_6\text{H}_4\text{C}(\text{O})\text{CH}_3\}\text{F}(\eta^2\text{-HD})(\text{P}^i\text{Pr}_3)_2$  (**4-d**), which has a H–D coupling constant of 1.7 Hz. According to eq 2, this value yields a hydrogen–hydrogen separation of 1.39 Å.

Complex **4** is another example of blocked rotation of the dihydrogen ligand on the NMR time scale. Line-shape analysis of the <sup>1</sup>H{<sup>31</sup>P} NMR spectra allows the calculation of the rate constants for the process at each temperature. The activation parameters obtained from the Eyring analysis (Figure 5) are  $\Delta H^\ddagger = 10.1 \pm 0.8$  kcal·mol<sup>-1</sup> and  $\Delta S^\ddagger = 1 \pm 2$  cal·mol<sup>-1</sup>·K<sup>-1</sup>. The value for the entropy of activation, close to 0, is in agreement with an intramolecular process, while the value for the enthalpy of activation lies in the range previously mentioned for the other blocked rotation processes.

It has been previously reported that the enthalpy of activation for the rotation of the H(01) and H(02)

hydrogen atoms in the complex  $\text{OsH}_3\{\text{C}_6\text{H}_4\text{C}(\text{O})\text{CH}_3\}(\text{P}^i\text{Pr}_3)_2$  is  $13.9 \pm 0.3$  kcal·mol<sup>-1</sup>. This value and those obtained from the spectra collected in Figure 4 show that the activation energy for the rotation of the H(01) and H(02) hydrogen atoms in the complexes of general

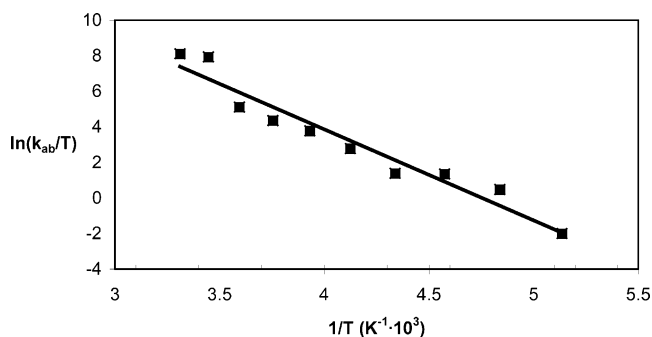


**Figure 5.** Eyring plot of the rate constants for the intramolecular hydride site exchange of the complex  $\text{Os}\{\text{C}_6\text{H}_4\text{C}(\text{O})\text{CH}_3\}\text{F}(\eta^2\text{-H}_2)(\text{P}^i\text{Pr}_3)_2$  (**4**).

formula  $\text{Os}\{\text{C}_6\text{H}_4\text{C}(\text{O})\text{CH}_3\}\text{L}(\eta^2\text{-H}_2)(\text{P}^i\text{Pr}_3)_2$  decreases in the same order as the strength of the H(01)–L interaction (**1** > **4** ≥ **3** > **2**). This suggests that the H(01)–L interaction makes a significant contribution to the rotation barrier of the dihydrogen in this type of compounds. In this context, it should be noted that the breaking of this interaction must be the first step to the rotation.

### Concluding Remarks

This study shows that, in *cis*-L–dihydrogen complexes of the type  $\text{Os}\{\text{C}_6\text{H}_4\text{C}(\text{O})\text{CH}_3\}\text{L}(\eta^2\text{-H}_2)(\text{P}^i\text{Pr}_3)_2$ , the elongated dihydrogen ligand undergoes a *cis* electrostatic attraction with the L ligand. This interaction increases in the sequence  $(\text{CH}_3)_2\text{CO}$  or  $\text{H}_2\text{O} < \text{Cl} \leq \text{F} < \text{H}$ , and it provokes a lengthening of the hydrogen–hydrogen bond and an increase in the rotation barrier of the elongated dihydrogen ligand. Thus, we show that the separation between the hydrogen atoms of the OsH<sub>2</sub> unit decreases in the sequence  $\text{H} > \text{F} > \text{Cl} > \text{H}_2\text{O}$  or  $(\text{CH}_3)_2\text{CO}$ , whereas the rotation barrier of the two hydrogen atoms increases in the sequence  $(\text{CH}_3)_2\text{CO} < \text{Cl} < \text{F} < \text{H}$ .

### Experimental Section

All reactions were carried out with rigorous exclusion of air using Schlenk-tube techniques. Solvents were dried by the usual procedures and distilled under argon prior to use. The starting material  $\text{OsH}_3\{\text{C}_6\text{H}_4\text{C}(\text{O})\text{CH}_3\}(\text{P}^i\text{Pr}_3)_2$  (**1**) was prepared by the published method.<sup>9</sup>

<sup>1</sup>H, <sup>19</sup>F, <sup>31</sup>P{<sup>1</sup>H}, and <sup>13</sup>C{<sup>1</sup>H} NMR spectra were recorded on a Varian UNITY 300, a Varian Gemini 2000, or a Bruker AXR 300 MHz instrument. Chemical shifts (expressed in parts per million) are referenced to residual solvent peaks (<sup>1</sup>H, <sup>13</sup>C{<sup>1</sup>H}), external H<sub>3</sub>PO<sub>4</sub> (<sup>31</sup>P{<sup>1</sup>H}), or external CFCl<sub>3</sub> (<sup>19</sup>F). Coupling constants,  $J$  and  $N$  ( $N = J_{\text{P-H}} + J_{\text{P'-H}}$  for <sup>1</sup>H and  $N = J_{\text{P-C}} + J_{\text{P'-C}}$  for <sup>13</sup>C{<sup>1</sup>H}) are given in hertz. Infrared spectra were run on a Perkin-Elmer 1730 spectrometer as solids (KBr pellet). C, H, and N analyses were carried out in a Perkin-Elmer 2400 CHNS/O analyzer. Mass spectral analyses were performed with a VG Austospec instrument. In the FAB<sup>+</sup> mode, ions were produced with the standard Cs<sup>+</sup> gun at ca. 30 kV, and 3-nitrobenzyl alcohol (NBA) was used in the matrix.

**Kinetic Analysis.** Complete line-shape analyses of the <sup>1</sup>H{<sup>31</sup>P} NMR spectra of the complex **4** were achieved using the program gNMR v4.1 (Cherwell Scientific Limited). The rate constants for various temperatures were obtained by fitting calculated to experimental spectra by full line-shape iterations.

(17) (a) Jalón, F. A.; Otero, A.; Manzano, B. R.; Villaseñor, E.; Chaudret, B. *J. Am. Chem. Soc.* **1995**, *117*, 10123. (b) Sabo-Etienne, S.; Chaudret, B.; el Makarim, H. A.; Barthelat, J.-C.; Daudey, J. P.; Ulrich, S.; Limbach, H.-H.; Moïse, C. *J. Am. Chem. Soc.* **1995**, *117*, 11602. (c) Antiñolo, A.; Carrillo-Hermosilla, F.; Fajardo, M.; García-Yuste, S.; Otero, A.; Camanyes, S.; Maseras, F.; Moreno, M.; Lledós, A.; Lluh, J. M. *J. Am. Chem. Soc.* **1997**, *119*, 6107. (d) Sabo-Etienne, S.; Rodríguez, V.; Donnadiu, B.; Chaudret, B.; el Makarim, H. A.; Barthelat, J.-C.; Ulrich, S.; Limbach, H.-H.; Moïse, C. *New J. Chem.* **2001**, *25*, 55.



The transverse relaxation time  $T_2$  was estimated at the lowest interval of temperatures using the resonances corresponding to the hydride ligands. The activation parameters  $\Delta H^\ddagger$  and  $\Delta S^\ddagger$  were calculated by least-squares fits of  $\ln(k/T)$  vs  $1/T$  (Eyring equation). Error analysis assumed a 10% error in the rate constant and 1 K in the temperature. Errors were computed by published methods.<sup>18</sup>

**Preparation of  $[\text{Os}\{\text{C}_6\text{H}_4\text{C}(\text{O})\text{CH}_3\}(\eta^2\text{-H}_2)\{\eta^1\text{-(CH}_3\text{)}_2\text{CO}\}(\text{P}^i\text{Pr}_3)_2]\text{BF}_4$  (**2**).** A red solution of **1** (100.0 mg, 0.158 mmol) in a mixture of 10 mL of diethyl ether and 5 mL of acetone was treated with  $\text{HBF}_4\cdot\text{OEt}_2$  (26  $\mu\text{L}$ , 0.190 mmol), stirred for 30 min at room temperature, and then evaporated to dryness. Subsequent addition of diethyl ether (5 mL) caused the precipitation of an orange solid, which was washed with further portions of diethyl ether and dried in vacuo. Yield: 99.6 mg (81%). Anal. Calcd for  $\text{C}_{29}\text{H}_{57}\text{BF}_4\text{O}_2\text{OsP}_2$ : C, 44.84; H, 7.40. Found: C, 45.20; H, 7.32. IR (KBr,  $\text{cm}^{-1}$ ):  $\nu(\text{OsH})$  2183 (s),  $\nu((\text{CH}_3)_2\text{CO})$  1711 (s),  $\nu(\text{CO})$  1657 (s),  $\nu(\text{BF})$  1050 (br).  $^1\text{H}$  NMR (300 MHz,  $\text{CD}_2\text{Cl}_2$ , 293 K):  $\delta$  7.76 and 7.74 (both d,  $J_{\text{H-H}} = 8.1$  Hz, 1H, Ph), 7.03 and 6.97 (both vt,  $J_{\text{H-H}} = 8.1$  Hz, 1H, Ph), 3.00 (s, 3H,  $\text{CH}_3$ ), 2.29 (br, 6H,  $(\text{CH}_3)_2\text{CO}$ ), 1.69 (m, 6H, PCH), 1.12 and 0.97 (both dvt,  $N = 13.2$  Hz,  $J_{\text{H-H}} = 6.7$  Hz, 18H, PCHCH<sub>3</sub>), -8.16 (br, 2H, OsH).  $^{31}\text{P}\{^1\text{H}\}$  NMR (121.42 MHz,  $\text{CD}_2\text{Cl}_2$ , 293 K):  $\delta$  12.2 (s).  $^{19}\text{F}$  NMR (282.33 MHz,  $\text{CD}_2\text{Cl}_2$ , 293 K):  $\delta$  -154.1 (br).  $^{13}\text{C}\{^1\text{H}\}$  NMR (75.42 MHz,  $\text{CD}_2\text{Cl}_2$ , 253 K):  $\delta$  220.0 (s,  $(\text{CH}_3)_2\text{CO}$ ), 208.9 (s, C=O), 175.9 (t,  $J_{\text{P-C}} = 5.3$  Hz, Os-C), 141.2 (s,  $\text{C}_{\text{ipso}}$ ), 143.5, 135.2, 132.6, and 120.4 (all s, Ph), 31.9 and 30.7 (both s,  $(\text{CH}_3)_2\text{CO}$ ), 25.2 (s,  $\text{CH}_3$ ), 24.3 (vt,  $N = 24.9$  Hz, PCH), 19.0 and 18.4 (both s, PCHCH<sub>3</sub>). MS (FAB<sup>+</sup>):  $m/z$  633 ( $\text{M}^+ - (\text{CH}_3)_2\text{CO}$ ).  $T_1(\text{min})$  (ms,  $\text{OsH}_2$ , 300 MHz,  $\text{CD}_2\text{Cl}_2$ , 193 K):  $48 \pm 1$  (-8.55 ppm, 2H).

**Preparation of  $[\text{Os}\{\text{C}_6\text{H}_4\text{C}(\text{O})\text{CH}_3\}\text{Cl}(\eta^2\text{-H}_2)(\text{P}^i\text{Pr}_3)_2]\text{BF}_4$  (**3**).** An orange solution of **2** (133.8 mg, 0.169 mmol) in 12 mL of methanol was treated with NaCl (11.9 mg, 0.203 mmol) and stirred for 25 min at room temperature. The solution was concentrated to ca. 1.5 mL, the solvent was decanted, and the solid was washed with further portions of methanol and dried in vacuo. A red solid was obtained. Yield: 85.7 mg (76%). Anal. Calcd for  $\text{C}_{26}\text{H}_{51}\text{ClOOsP}_2$ : C, 46.80; H, 7.70. Found: C, 46.66; H, 7.37. IR (KBr,  $\text{cm}^{-1}$ ):  $\nu(\text{OsH})$  2187 (s),  $\nu(\text{CO})$  1592 (s).  $^1\text{H}$  NMR (300 MHz,  $\text{C}_7\text{D}_8$ , 293 K):  $\delta$  8.13 (d,  $J_{\text{H-H}} = 7.5$  Hz, 1H, Ph), 7.39 (dd,  $J_{\text{H-H}} = 7.5$  Hz,  $J_{\text{H-H}} = 1.5$  Hz, 1H, Ph), 6.87 (vtd,  $J_{\text{H-H}} = 7.5$  Hz,  $J_{\text{H-H}} = 1.5$  Hz, 1H, Ph), 6.76 (vt,  $J_{\text{H-H}} = 7.5$  Hz, 1H, Ph), 2.60 (t,  $J_{\text{P-H}} = 1.2$  Hz, 3H,  $\text{CH}_3$ ), 2.45 (m, 6H, PCH), 1.25 and 1.08 (both dvt,  $N = 12.6$  Hz,  $J_{\text{H-H}} = 6.9$  Hz, 18H, PCHCH<sub>3</sub>), -8.76 (t,  $J_{\text{P-H}} = 11.7$  Hz, 2H, OsH).  $^{31}\text{P}\{^1\text{H}\}$  NMR (121.42 MHz,  $\text{C}_6\text{D}_6$ , 293 K):  $\delta$  10.0 (s).  $^{13}\text{C}\{^1\text{H}\}$  NMR (75.42 MHz,  $\text{C}_6\text{D}_6$ , 293 K):  $\delta$  205.6 (s, C=O), 187.8 (t,  $J_{\text{P-C}} = 5.3$  Hz, Os-C), 142.8 (s,  $\text{C}_{\text{ipso}}$ ), 145.2, 133.0, 131.5, and 117.9 (all s, Ph), 24.0 (vt,  $N = 24.1$  Hz, PCH), 22.7 (s,  $\text{CH}_3$ ), 19.2 and 18.9 (both s, PCHCH<sub>3</sub>). MS (FAB<sup>+</sup>):  $m/z$  666 ( $\text{M}^+ - \text{H}_2$ ).  $T_1(\text{min})$  (ms,  $\text{OsH}_2$ , 300 MHz,  $\text{C}_7\text{D}_8$ , 193 K):  $50 \pm 1$  (-9.08 ppm, 1H),  $50 \pm 1$  (-9.28 ppm, 1H).

$[\text{Os}\{\text{C}_6\text{H}_4\text{C}(\text{O})\text{CH}_3\}\text{Cl}(\eta^2\text{-HD})(\text{P}^i\text{Pr}_3)_2]$  was obtained by the following procedure. A suspension of **1** (20 mg, 0.032 mmol) in 3 mL of  $\text{MeOD-}d_4$  was treated first with  $\text{HBF}_4\cdot\text{D}_2\text{O}$  (4  $\mu\text{L}$ , 0.032 mmol). After 20 min, a solution of NaCl (2 mg, 0.035 mmol) in 3 mL of  $\text{MeOD-}d_4$  was added to the orange solution obtained. The red solid that formed was separated by decantation and dried in vacuo.  $^1\text{H}$  NMR (300 MHz,  $\text{C}_6\text{D}_6$ , 293 K):  $\delta$  -8.74 (tt (1:1:1),  $J_{\text{H-P}} = 11.7$  Hz,  $J_{\text{H-D}} = 4.5$  Hz, 1H, OsH).

**Preparation of  $[\text{Os}\{\text{C}_6\text{H}_4\text{C}(\text{O})\text{CH}_3\}\text{F}(\eta^2\text{-H}_2)(\text{P}^i\text{Pr}_3)_2]$  (**4**).** An orange solution of **2** (181.4 mg, 0.229 mmol) in 15 mL of tetrahydrofuran was treated with  $\text{CsF}$  (52.0 mg, 0.342 mmol) and stirred for 19 h at room temperature. Then, the solvent was removed and toluene (15 mL) was added to filter the ionic

**Table 4. Crystal Data and Data Collection and Refinement Parameters for **2** and **4****

	<b>2</b>	<b>4</b>
Crystal Data		
formula	$\text{C}_{29}\text{H}_{57}\text{BF}_4\text{O}_2\text{OsP}_2$	$\text{C}_{26}\text{H}_{51}\text{FOOsP}_2$
mol wt	776.70	650.81
color, habit	red, irregular block	red, irregular block
symmetry, space group	orthorhombic, $P2_12_12_1$	orthorhombic, $Pbca$
<i>a</i> , Å	12.1214(12)	17.319(2)
<i>b</i> , Å	15.8529(15)	15.1840(18)
<i>c</i> , Å	18.2420(18)	22.515(3)
<i>V</i> , Å <sup>3</sup>	3505.4(6)	5920.9(13)
<i>Z</i>	4	8
<i>D</i> <sub>calcd</sub> , g cm <sup>-3</sup>	1.472	1.460
Data Collection and Refinement		
diffractometer	Bruker Smart APEX	
$\lambda(\text{Mo K}\alpha)$ , Å	0.710 73	
monochromator	graphite oriented	
scan type	$\omega$ scans	
$\mu$ , mm <sup>-1</sup>	3.773	4.436
$2\theta$ range, deg	3–56	
temp, K	173	
no. of data collected	23 168	37 761
no. of unique data	8301 ( $R_{\text{int}} = 0.0767$ )	7243 ( $R_{\text{int}} = 0.1707$ )
no. of params/restraints	371/28	299/35
$R1^a$ ( $F^2 > 2\sigma(F^2)$ )	0.0372	0.0533
$wR2^b$ (all data)	0.0635	0.0935
$S^c$ (all data)	0.725	0.708

<sup>a</sup>  $R1(F) = \sum ||F_o| - |F_c|| / \sum |F_o|$ . <sup>b</sup>  $wR2(F^2) = \{\sum [w(F_o^2 - F_c^2)^2] / \sum [w(F_o^2)^2]\}^{1/2}$ . <sup>c</sup>  $\text{GOF} = S = \{\sum [(F_o^2 - F_c^2)^2] / (n - p)\}^{1/2}$ , where *n* is the number of reflections and *p* is the number of refined parameters.

salts. The resulting solution was dried in vacuo, and pentane was added to afford a red solid, which was washed with pentane at -78 °C and dried in vacuo. Yield: 85.1 mg (57%). Anal. Calcd for  $\text{C}_{26}\text{H}_{51}\text{FOOsP}_2$ : C, 47.98; H, 7.90. Found: C, 47.58; H, 7.77. IR (KBr,  $\text{cm}^{-1}$ ):  $\nu(\text{OsH})$  2147 (s),  $\nu(\text{CO})$  1588 (s).  $^1\text{H}$  NMR (300 MHz,  $\text{C}_7\text{D}_8$ , 293 K):  $\delta$  8.08 (d,  $J_{\text{H-H}} = 7.5$  Hz, 1H, Ph), 7.46 (dd,  $J_{\text{H-H}} = 7.5$  Hz,  $J_{\text{H-H}} = 1.5$  Hz, 1H, Ph), 6.76 (vtd,  $J_{\text{H-H}} = 7.5$  Hz,  $J_{\text{H-H}} = 1.5$  Hz, 1H, Ph), 6.71 (vt,  $J_{\text{H-H}} = 7.5$  Hz, 1H, Ph), 2.69 (t,  $J_{\text{P-H}} = 1.2$  Hz, 3H,  $\text{CH}_3$ ), 2.22 (m, 6H, PCH), 1.19 and 1.17 (both dvt,  $N = 13.2$  Hz,  $J_{\text{H-H}} = 7.2$  Hz, 18H, PCHCH<sub>3</sub>), -7.71 (dt,  $J_{\text{F-H}} = 18.3$  Hz,  $J_{\text{P-H}} = 12.6$  Hz, 2H, OsH).  $^{31}\text{P}\{^1\text{H}\}$  NMR (121.42 MHz,  $\text{C}_6\text{D}_6$ , 293 K):  $\delta$  19.4 (d,  $J_{\text{F-P}} = 29.9$  Hz).  $^{19}\text{F}$  NMR (282.33 MHz,  $\text{C}_6\text{D}_6$ , 293 K):  $\delta$  -360.4 (tt,  $J_{\text{F-P}} = 26.6$  Hz,  $J_{\text{F-H}} = 18.3$  Hz, OsF).  $^{13}\text{C}\{^1\text{H}\}$  NMR (75.42 MHz,  $\text{C}_6\text{D}_6$ , 293 K):  $\delta$  203.4 (s, C=O), 190.3 (d,  $J_{\text{F-C}} = 29.9$  Hz, Os-C), 142.9 (s,  $\text{C}_{\text{ipso}}$ ), 147.2, 147.1, 132.2, and 131.9 (all s, Ph), 23.7 (vt,  $N = 23.0$  Hz, PCH), 22.9 (s,  $\text{CH}_3$ ), 19.3 (s, PCHCH<sub>3</sub>). MS (FAB<sup>+</sup>):  $m/z$  638 ( $\text{M}^+ - \text{CH}_3$ , +H).  $T_1(\text{min})$  (ms,  $\text{OsH}_2$ , 300 MHz,  $\text{C}_7\text{D}_8$ , 223 K):  $64 \pm 2$  (-7.49 ppm, 2H).

$[\text{Os}\{\text{C}_6\text{H}_4\text{C}(\text{O})\text{CH}_3\}\text{F}(\eta^2\text{-HD})(\text{P}^i\text{Pr}_3)_2]$  was obtained from **4** in  $\text{CD}_3\text{OD-}d_2\text{O}$  (2:0.1 mL) in 2 days.  $^1\text{H}$  NMR (300 MHz,  $\text{CD}_3\text{OD}$ , 293 K):  $\delta$  -7.65 (dtt (1:1:1),  $J_{\text{H-F}} = 18.3$  Hz,  $J_{\text{H-P}} = 12.6$  Hz,  $J_{\text{H-D}} = 1.7$  Hz, 1H, OsH).

**X-ray Analysis of **2** and **4**.** Two irregular green crystals of size 0.16 × 0.08 × 0.02 mm (**2**) and 0.12 × 0.10 × 0.06 mm (**4**) were mounted on a Bruker Smart APEX CCD diffractometer at 173.0(2) K equipped with a normal-focus, 2.4 kW sealed tube source (molybdenum radiation,  $\lambda = 0.710 73$  Å) operating at 50 kV and 40 mA (**2**) or 30 mA (**4**). Data were collected over the complete sphere by a combination of four sets. Each frame exposure time was 10 s, covering 0.3° in  $\omega$ . The cell parameters were determined and refined by least-squares fits of 3543 (**2**) and 1336 (**4**) collected reflections. The first 100 frames were collected at the end of the data collection to monitor crystal decay. Absorption correction was performed

(18) Morse, P. M.; Spencer, M. D.; Wilson, S. R.; Girolami, G. S. *Organometallics* **1994**, *13*, 1646.

with the SADABS<sup>19</sup> program. Lorentz and polarization corrections were also performed. The structures were solved by Patterson and Fourier methods and refined by full-matrix least squares using the Bruker SHELXTL<sup>20</sup> program, package minimizing  $w(F_o^2 - F_c^2)^2$ . The BF<sub>4</sub> anion of **2** was observed to be disordered and was refined as two moieties with isotropic atoms, complementary occupancy factors, and restrained geometry. A triisopropylphosphine group of complex **4** was also observed to be disordered and was refined with complementary isopropyl groups and restrained geometry. The non-disordered non-hydrogen atoms were anisotropically refined. The hydrogen atoms were observed or calculated and refined riding on the bonded carbon atoms. The hydride ligands were observed in the difference Fourier maps, but they could not be refined properly. A model with fixed bond lengths to the osmium atoms and thermal parameters was used. Weighted *R* factors (*R*<sub>w</sub>) and goodness of fit values (*S*) are based on *F*<sup>2</sup>; conventional *R* factors are based on *F*. Crystal data and details of the data collection and refinement are given in Table 4.

**Computational Details.** DFT optimizations were carried out with the Gaussian98<sup>21</sup> series of programs using the B3LYP functional.<sup>22</sup> A quasi-relativistic effective core potential operator was used to represent the innermost electrons of the osmium atom.<sup>23</sup> The basis set for the osmium atom was that associated with the pseudopotential with a standard valence double- $\zeta$  LANL2DZ contraction.<sup>21</sup> A 6-31G(d) basis set was used for the phosphorus, fluoride, oxygen, and chlorine atoms.<sup>24</sup> Hydrogens directly attached to the metal were described using a 6-311G(p) basis set,<sup>24</sup> while a 6-31G basis set was used for the rest of the hydrogens.<sup>25</sup> A 6-31G basis set<sup>25</sup> was also used for all of the carbon atoms, except for those involved in the bonding with the osmium atom, which were described using a 6-31G(d) basis set.

(19) Blessing, R. H. *Acta Crystallogr., Sect. A* **1995**, *51*, 33. SADABS, Area-Detector Absorption Correction; Bruker-AXS, Madison, WI, 1996.

(20) SHELXTL Package, v. 6.10; Bruker-AXS, Madison, WI, 2000. Sheldrick, G. M. SHELXS-86 and SHELXL-97; University of Göttingen, Göttingen, Germany, 1997.

**Acknowledgment.** Financial support from the MCYT of Spain (Proyect BQU2002-00606, PPQ2000-0488-P4-02, and BQU 2002-04110-CO2-02) is acknowledged. The use of computational facilities of the Centre de Supercomputació de Catalunya is gratefully appreciated. P.B. thanks the "Ministerio de Educación, Cultura y Deporte" for her grant.

**Supporting Information Available:** Tables of positional and displacement parameters, crystallographic data, and bond lengths and angles. This material is available free of charge via the Internet at <http://pubs.acs.org>.

OM0342513

(21) Frisch, M. J.; Trucks, G. W.; Schlegel, H. B.; Scuseria, G. E.; Robb, M. A.; Cheeseman, J. R.; Zakrzewski, V. G.; Montgomery, J. A., Jr.; Stratmann, R. E.; Burant, J. C.; Dapprich, S.; Millam, J. M.; Daniels, A. D.; Kudin, K. N.; Strain, M. C.; Farkas, O.; Tomasi, J.; Barone, V.; Cossi, M.; Cammi, R.; Mennucci, B.; Pomelli, C.; Adamo, C.; Clifford, S.; Ochterski, J.; Petersson, G. A.; Ayala, P. Y.; Cui, Q.; Morokuma, K.; Malick, D. K.; Rabuck, A. D.; Raghavachari, K.; Foresman, J. B.; Cioslowski, J.; Ortiz, J. V.; Stefanov, B. B.; Liu, G.; Liashenko, A.; Piskorz, P.; Komaromi, I.; Gomperts, R.; Martin, R. L.; Fox, D. J.; Keith, T.; Al-Laham, M. A.; Peng, C. Y.; Nanayakkara, A.; Gonzalez, C.; Challacombe, M.; Gill, P. M. W.; Johnson, B.; Chen, W.; Wong, M. W.; Andres, J. L.; Gonzalez, C.; Head-Gordon, M.; Replogle, E. S.; Pople, J. A. Gaussian 98, revision A.6; Gaussian Inc., Pittsburgh, PA, 1998.

(22) (a) Lee, C.; Yang, W.; Parr, R. G. *Phys. Rev. B* **1988**, *37*, 785. (b) Becke, A. D. *J. Chem. Phys.* **1993**, *98*, 5648. (c) Stephens, P. J.; Devlin, F. J.; Chabalowski, C. F.; Frisch, M. J. *J. Phys. Chem.* **1994**, *98*, 11623.

(23) Hay, P. J.; Wadt, W. R. *J. Chem. Phys.* **1985**, *82*, 299.

(24) (a) Hehre, W. J.; Ditchfield, R.; Pople, J. A. *J. Chem. Phys.* **1972**, *56*, 2257. (b) Hariharan, P. C.; Pople, J. A. *Theor. Chim. Acta* **1973**, *28*, 213. (c) Francl, M. M.; Pietro, W. J.; Hehre, W. J.; Binkley, J. S.; Gordon, M. S.; DeFrees, D. J.; Pople, J. A. *J. Chem. Phys.* **1982**, *77*, 3654.

(25) Höllwarth, A.; Böhme, M.; Dapprich, S.; Ehlers, A. W.; Gobbi, A.; Jonas, V.; Köhler, K. F.; Stegman, R.; Veldkamp, A.; Frenking, G. *Chem. Phys. Lett.* **1993**, *208*, 237.